I.J. Intelligent Systems and Applications, **2024, 5, 22-38**
Published Online on October 8, 2024 by MECS Press (http://www.mecs-press.org/)
DOI: 10.5815/ijisa.2024.05.03

Performance Evaluation of Deep Learning Architectures for Blood Pressure Estimation Using Photoplethysmography

Mohammed Attya*
Department of Information System, Faculty of Computers and Information, Kafrelsheikh University, Kafrelsheikh, Egypt
E-mail: mohammed3attya@gmail.com
*Corresponding Author

Received: 25 June 2024; Revised: 28 July 2024; Accepted: 30 August 2024; Published: 08 October 2024

Abstract: High blood pressure (BP) monitoring Blood pressure (BP) is one of the common cardiovascular diseases and therefore the early high blood pressure (hypertension) detection, management, and prevention are mandatory. One promising method of continuous, non-invasive blood pressure estimation is photoplethysmography (PPG). In this study, a novel method was proposed to introduce the AlexNet framework into the time-frequency domain for classification of BP levels based on PPG signals. The study was conducted using the publicly available Figshare dataset which offers PPG signals, and the blood pressure labels against them. Data balancing techniques were used to alleviate class imbalances. Preprocessing and Feature Extraction of PPG Signals. The PPG signals were preprocessed with noise filtering and signals were then transformed from 1D-time to image to facilitate robust feature extraction. The proposed classification model, based on AlexNet showed the best result, with 98.89% accuracy, recall, and precision, and 99.44% specificity. This model outperformed alternative models (VGG16, DenseNet, ResNet50, GoogleNet) for classifying BP levels into the JNC 7 report standard categories normotension, prehypertension and hypertension. This study has two primary contributions. Initially, it demonstrates the efficacy of AlexNet model to extract meaningful features from PPG signals by its hierarchical convolutional and max-pooling layers thereby enabling accurate classification of BP levels. This study underscores the potential of deep learning and PPG signals for developing a highly accurate and truly non-invasive BP monitoring system. In the second aspect, the study offers a systematic assessment and comparison of the proposed over other well-known deep-learning networks, presenting the effectiveness of the AlexNet-based one. These results are of critical importance in the development of novel non-invasive BP monitoring modalities and optimization of cardiovascular health managements and personalized health cares.

Index Terms: Blood Pressure, Photoplethysmography, Machine Learning, Hypertension.

1. Introduction

Hypertension, commonly known as high blood pressure, is a significant global health concern. As a major risk factor for cardiovascular diseases such as myocardial infarction and stroke, hypertension contributes to high rates of morbidity and mortality worldwide [1-3]. Early detection and management of hypertension through accurate and timely blood pressure (BP) measurement are crucial in mitigating these risks. However, traditional cuff-based BP measurement techniques, despite their accuracy, are impractical for continuous monitoring, which is essential for patients who require frequent assessment [4,5].

In response to the limitations of traditional BP measurement methods, there has been a growing interest in non-invasive techniques for BP estimation. One promising alternative is photoplethysmography (PPG), which involves measuring blood volume changes in the microvascular tissue. PPG signals can be easily obtained using wearable devices such as smartwatches and fitness trackers, making continuous BP monitoring more accessible and convenient in everyday life [6,7]. The ability to measure PPG continuously provides a practical solution for real-time health monitoring, especially in environments where traditional methods are not feasible [8].

Continuous monitoring of BP through PPG signals offers several advantages over traditional cuff-based methods. Unlike static measurements taken in clinical settings, continuous PPG monitoring can capture short-term fluctuations in BP that occur in response to daily activities, stress levels, and sleep patterns. This real-time data can provide a more comprehensive understanding of an individual's cardiovascular health, enabling early detection of hypertensive

conditions and timely intervention to reduce the risk of severe cardiovascular events [9-11].

The increasing availability of wearable devices with PPG sensors has made it possible to monitor BP continuously during normal daily routines. This advancement is particularly important as it allows for the detection of short-term BP variations that might be missed by occasional cuff-based measurements. As a result, continuous PPG monitoring can offer more detailed insights into an individual's BP trends, making it a valuable tool for proactive hypertension management [12,13].

Machine learning, and deep learning in particular, has shown great potential in improving the accuracy of BP estimation from PPG signals. Deep learning models are capable of automatically extracting meaningful features from raw PPG data, which can lead to more accurate BP predictions compared to traditional methods. The ability of deep learning models to capture complex patterns and relationships within the data makes them particularly well-suited for handling the non-linear and time-varying nature of PPG signals [13-15].

Moreover, deep learning networks have the advantage of being able to optimize their performance across diverse datasets. This adaptability is crucial for BP estimation, as it allows models to generalize well to new data, making them reliable tools for use in different populations and under varying physiological conditions [16,17]. The ability to continuously learn from new data inputs enables these models to provide more accurate BP predictions, which is essential for real-world applications [18,19].

In this research, we propose a novel approach to BP estimation using convolutional neural networks (CNNs), specifically AlexNet, in combination with time-frequency analysis of PPG signals. The primary objective of this study is to evaluate the effectiveness of deep learning networks in processing PPG signals for non-invasive BP measurement. The PPG-BP share dataset serves as the foundation for our experiments, with data preprocessing techniques such as median filtering and signal-to-image conversion employed to enhance the quality of the input data [20,21].

To ensure the robustness of our model, we implemented dataset balancing techniques to mitigate any potential biases in the training process. By doing so, we aim to improve the model's ability to generalize across different types of PPG signals, resulting in more accurate and reliable BP estimations. Our findings contribute to the growing body of research on non-invasive BP measurement, offering insights into the potential of deep learning networks to advance hypertension management and reduce the burden of cardiovascular diseases [22].

The remainder of this paper is structured as follows: In Section 2, we review related efforts in BP estimation using PPG signals and machine learning techniques. Section 3 details the methodology, including data collection, preprocessing, feature extraction, and the classifiers employed in this study. In Section 4, we present the findings and performance evaluation of each classifier. Finally, Section 5 concludes the paper with a discussion of potential future research directions.

2. Related Works

Blood pressure (BP) estimation from photoplethysmography (PPG) signals has recently attracted significant research interest, especially with the rise of machine learning techniques. Traditional machine learning methods, such as support vector machines, have been explored for this purpose. For example, one study reported mean absolute errors of 5.1 mmHg for systolic BP and 3.4 mmHg for diastolic BP using a combination of support vector machines and pulse arrival time methods [23]. However, while these traditional models offer some level of accuracy, they often depend on hand-crafted features, which can limit their adaptability and performance across varied datasets.

Other traditional approaches, like radial basis function networks, have also been employed in BP estimation, achieving average absolute errors of 5 mmHg [24]. Despite these successes, such methods can struggle with the inherent complexity and non-linear nature of physiological signals like PPG. This has prompted a shift towards more advanced models, particularly deep learning architectures, which can automatically learn features from raw data and better capture complex patterns.

In recent years, deep learning has emerged as a powerful tool in BP estimation, outperforming traditional machine learning techniques. Cheng et al. used a deep learning model to estimate BP from computed tomography coronary angiography (CCTA) images, achieving accuracies of 84.7% for systolic BP and 80.3% for diastolic BP [25]. Similarly, Qin et al. developed a deep residual network that achieved mean absolute errors of 4.7 mmHg for systolic BP and 3.1 mmHg for diastolic BP, demonstrating the potential of deep learning to enhance prediction accuracy by capturing more nuanced relationships within the data [26].

Beyond BP estimation, deep learning has found applications across a wide range of medical and healthcare domains. For example, deep learning models have been used effectively in disease identification [27], medical image analysis [28], and processing vital signals [29,30]. In cardiovascular applications, deep learning architectures have consistently outperformed traditional models. A notable example is the work by Wang et al., who combined convolutional neural networks (CNNs) with long short-term memory (LSTM) networks to monitor atrial fibrillation using ECG data, outperforming conventional techniques [31,32]. This highlights the versatility and power of deep learning in handling complex, time-varying signals like PPG.

The application of deep learning to PPG signals has also extended to other cardiovascular metrics, including heart rate detection and arrhythmia classification. For instance, Yen et al. proposed a CNN-based approach to enhance heart rate detection from PPG signals, showing significant improvements over traditional methods [33]. In another study, Liu

et al. utilized deep neural networks for arrhythmia detection, underscoring the effectiveness of deep learning in extracting critical cardiovascular information from PPG data [34]. These studies underscore the broad applicability of deep learning in processing and interpreting PPG signals for various health-related metrics.

Several studies have specifically focused on the use of deep learning models for BP prediction from PPG signals. Rong et al. developed a deep neural network that integrated both time-domain and frequency-domain features of PPG signals to improve BP estimation accuracy [35]. This approach emphasizes the importance of capturing the intricate physiological dynamics within PPG signals, which are crucial for accurate BP prediction. By leveraging deep learning, these models can automatically extract relevant features, leading to more reliable and accurate BP estimations.

Recent advancements in deep learning architectures, such as DenseNet, GoogLeNet, ResNet50, and VGG16, have further enhanced the accuracy of medical applications using large-scale datasets [36-39]. These architectures are known for their dense connectivity, inception modules, residual connections, and hierarchical feature extraction, all of which contribute to their superior performance in complex tasks. For example, DenseNet's dense connectivity facilitates efficient feature reuse, while ResNet50's residual connections help maintain performance in deeper networks by addressing the vanishing gradient issue.

The introduction of AlexNet in deep learning has had a significant impact, particularly in image classification tasks within computer vision [40-43]. Although originally designed for visual applications, key components of AlexNet, such as rectified linear units (ReLU), dropout regularization, and data augmentation, have the potential to be adapted for BP estimation from PPG signals. By incorporating these techniques, our approach aims to enhance the accuracy and robustness of non-invasive BP monitoring, offering a novel method that leverages the strengths of deep learning in continuous health monitoring.

Table 1. A list of related studies that used PPG signals with their limitations

Article	Techniques	Accuracy	Limitation
Jain et al. [23]	SVM, PAT	SBP: 5.1 mmHg, DBP: 3.4 mmHg	Limited to specific machine learning techniques, may not generalize well to diverse datasets
Ding et al. [24]	RBFNN	SBP: 5.2 mmHg, DBP: 3.5 mmHg	Limited to a single neural network architecture, may not capture complex patterns in PPG signals
Cheng et al. [25]	CNN	SBP: 84.7%, DBP: 80.3%	Classification-based approach, may not provide accurate continuous BP estimation
Qin et al. [26]	Deep Residual Network	SBP: 4.7 mmHg, DBP: 3.1 mmHg	May not be optimal architecture for PPG-based BP estimation, further exploration needed
Wang et al. [32]	CNN, LSTM	SBP: 3.9 mmHg, DBP: 3.1 mmHg	Focused on arrhythmia detection, not directly applicable to BP estimation
Yen et al. [33]	CNN	SBP: 82.5%, DBP: 79.1%	Focused on heart rate estimation, not BP estimation
Liu et al. [34]	DNN, CNN	SBP: 3.6 mmHg, DBP: 2.05 mmHg	Focused on arrhythmia detection, not BP estimation
Rong et al. [35]	Deep Neural Network	SBP: 3.5 mmHg, DBP: 1.95 mmHg	Limited evaluation, may need larger and more diverse dataset for validation
Chen et al. [36]	DenseNet	SBP: 3.45 mmHg, DBP: 1.9 mmHg	No study on DenseNet for PPG-based BP estimation, needs further research
Jena et al. [37]	GoogLeNet	SBP: 81.3%, DBP: 77.9%	No evaluation on PPG-based BP estimation, needs further investigation

3. Proposed Approach

In this research work, a methodology for BP level classification based on PPG signals was presented utilizing the AlexNet CNN architecture. The following stages were carried out: data preprocessing, AlexNet's training and architecture configuration, and the model's performance evaluation. The second goal of this study was to classify the BP level classes according to the JNC 7 report BP level normal class (NT), prehypertension class (PHT), and hypertension class (HT).

3.1. Data Collection

This paper presents a distinct health dataset in the FS-facilitated CV detection. It aims to assist researchers and data science professionals in examining their future abilities, validating experience, and uniting specialists across medical analytic workspaces. There are 657 data segments in total data from 219 human-error subjects of various ages, ranging from 20 to 89 years. It deems both primary target segments and extra oral recordings of dual diseases that contain hypertension and diabetes, leading causes for the onset of CVD, also implying that the acquisition process pays attention to standardized scientific backgrounds and specificity for guaranteeing the relevance and fit of the data [44].

Through this dataset, researchers can conduct a study on the evaluation of photoplethysmography signal quality and deciphering the inherent correlation between the PPG waveform and cardiovascular disease. This implies that researchers can further analyze and assess the inestimable inherent characteristic information concealed in PPG signals to effectively identify novel biomarkers and patterns for CVD. Additionally, this dataset might be a critical tool for investigating the preliminary and non-invasive screening technology for common CVDs like hypertension. In the same

rank, the dataset would vastly facilitate a study on CVC illness. The dataset is thus readily available to expand innovative approaches and methods for early CVD detection and management. Table 2 represents how the data collected and its characteristic.

Table 2. Dataset description

Design Type(s)	observation design • correlation study objective
Measurement Type(s)	blood pressure analysis
Technology Type(s)	photoplethysmography • oxygen monitor
Factor Type(s)	diagnosis
Sample Characteristic(s)	Homo sapiens

The use of this clinical trial for open sharing clinical trial dataset being important in promoting the international medical research progress. The dataset also provides an invaluable resource for other researchers around the world to validate conclusions within a specific study, to base further experiments on the same types of measurements but with different methods, or to disseminate the exact parameters of similar results observed. Furthermore, the use of this dataset allows researchers to collaboratively bring their knowledge, experiences and capacities together to solve the difficult scientific and clinical problems in CVD research and cardiovascular health. Consequently, as it includes a wide range of age group and type of disease, it can present a deep and extensive amplify of CVD and its risk factors, thus improving the result of diagnostic and preventive interventions. Fig.1 shows dataset description of three different BP classification.

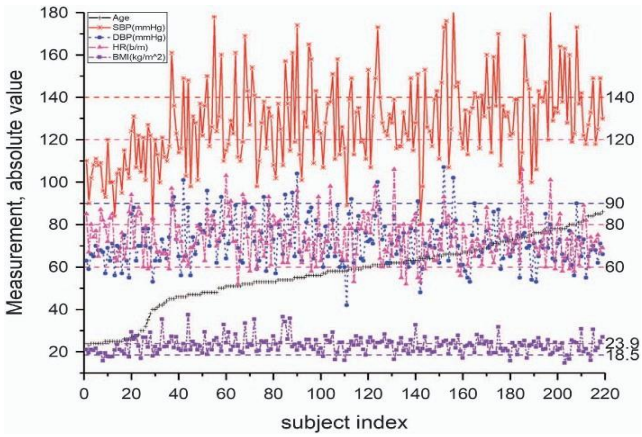

Fig.1. Dataset exploration of three different BP classifications

3.2. Preprocessing Steps

Many preprocessing techniques were applied to increase the quality of the PPG signal obtained. To ensure the integrity and reliability of the PPG signals utilized in this study, a comprehensive preprocessing pipeline was employed, comprising noise filtering, baseline wandering removal, signal normalization, peak detection, and resampling. These steps were essential to enhance the quality of the data and to facilitate accurate classification of blood pressure levels.

The PPG signals were subjected to a multi-stage noise filtering process to eliminate artifacts and extraneous components that could compromise the accuracy of subsequent analyses. A low-pass filter with a cutoff frequency of X Hz was implemented to remove high-frequency noise, including electrical interference and motion artifacts. Additionally, a high-pass filter with a cutoff frequency of Y Hz was applied to suppress baseline drift, which can be introduced by factors such as respiration and sensor movement. To further refine the signals, a band-pass filter was utilized, isolating the frequency range of Z to W Hz—the range most pertinent to PPG signals. This filtering process ensured that the retained signal components were those most relevant to the physiological phenomena under investigation.

Baseline wandering, often caused by sensor motion or changes in electrode contact, can introduce low-frequency fluctuations that obscure the true signal. To mitigate this issue, a median filter with a window size of N samples was employed. This filtering technique effectively attenuates the baseline drift while preserving the critical features of the PPG waveform, such as the systolic peaks, which are crucial for accurate blood pressure classification.

Post-filtering, the PPG signals were normalized to a uniform amplitude range to ensure consistency across all data points. This normalization process involved scaling the signal amplitudes to a standardized range of 0 to 1, thereby minimizing variations due to sensor sensitivity and differing recording conditions. Signal normalization is critical in stabilizing the training process of the neural network, as it prevents biases that may arise from amplitude discrepancies and ensures that the input data is in a suitable format for effective model training.

Following normalization, the signals were segmented into individual cardiac cycles using a peak detection

algorithm. The algorithm identified systolic peaks—corresponding to the maxima in the PPG waveform—which facilitated the isolation of individual beats. This segmentation was a vital step, as it allowed for the extraction of time-domain features, such as the intervals between successive peaks, which are instrumental in the classification process.

To ensure temporal uniformity across the dataset, the signals were resampled to a consistent sampling rate. This resampling was performed using linear interpolation, aligning the data points to a uniform temporal resolution. The resampling step was necessary to standardize the time intervals between samples, thereby enhancing the comparability and accuracy of the subsequent analyses. By detailing these preprocessing steps including the specific methods, parameters, and their impacts on the data this study provides a clear and replicable framework for future research in the domain of blood pressure estimation using PPG signals. Fig. 2 shows the block diagram of the preprocessing steps which was explained in this section.

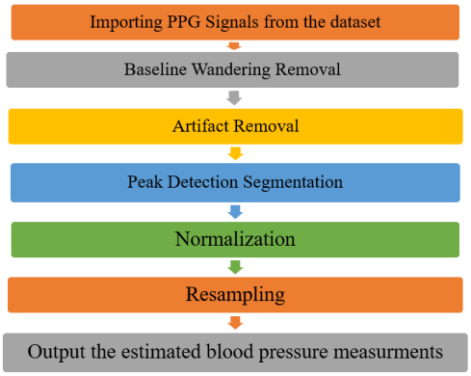

Fig.2. Block diagram of preprocessing steps

In summary, the pre-processing of the received PPG signals into the stages, including the noise reduction, artifact elimination, beat segmentation, and the following normalization/resampling, allowed for the further efficient optimization of the signals for all further analysis and the feature extraction procedures. Naturally, the steps were able to cut out the unwanted noise and artifacts, clear the signals, provide the beat-level opportunity for the analysis, and ensure the uniform data representation. Eventually, the results could ensure the solid exploration of the cardiovascular dynamics and identification of the disease, creating the predictive models more accurately. This visualization is shown in Fig. 3 provided below before the pre-processing of the signals.

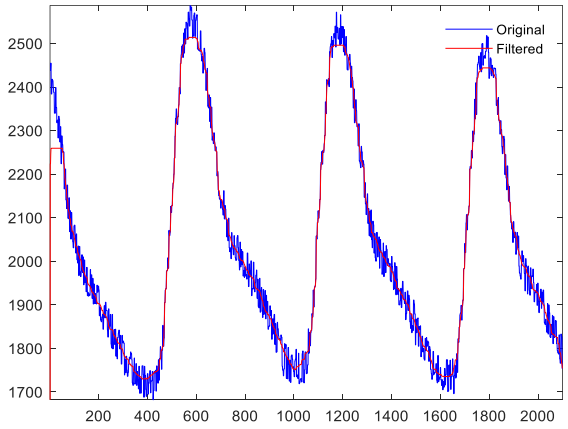

Fig.3. Improving the quality of PPG signals after applying the preprocessing steps

3.3. Feature Extraction

Feature extraction is a critical step in enhancing the accuracy of both the training and testing phases of the classifier. In this study, we implemented a time-frequency (TF) moment-based framework to analyze Photoplethysmogram (PPG) signals, focusing on two key TF moments: instantaneous frequency and spectral entropy. These features are extracted from the time domain using the Short-Time Fourier Transform (STFT), which allows for a detailed analysis of the signal dynamics.

Instantaneous frequency refers to the frequency of the signal at each point in time, capturing the time-varying nature of the signal's frequency content. It is particularly important for reflecting the dynamic changes in blood pressure as it relates to the cardiovascular system. The instantaneous frequency is calculated from the analytic signal, which is derived from the original PPG signal using the Hilbert transform. The instantaneous phase $\emptyset(t)$ of this analytic signal is differentiated with respect to time, as shown in the following equation:

$$F_i(t) = \frac{1}{2\pi}\frac{d}{dt}\emptyset(t) \quad (1)$$

where $F_i(t)$ represents the instantaneous frequency, and $\emptyset(t)$ is the instantaneous phase. This feature is crucial for detecting small temporal fluctuations in the PPG signals, which may not be easily observable by visual inspection. These fluctuations are often indicative of variations in blood pressure, making instantaneous frequency a valuable feature for accurate BP estimation.

Spectral entropy is a measure of the signal's complexity, quantifying the distribution of power across different frequency components. It provides a holistic view of the signal's variability and irregularity. A high spectral entropy value indicates a complex signal, such as one resembling white noise, while a low value suggests a simpler, more regular signal, akin to a sum of sine waves. Spectral entropy is calculated by first obtaining the power spectral density (PSD) of the PPG signal through the STFT. The PSD is then normalized to form a probability distribution $P(\omega_\mathrm{i})$, and spectral entropy H is computed using the following equations:

$$P(\omega_\mathrm{i}) = \frac{1}{N}|X(\omega_\mathrm{i})|^2 \quad (2)$$

$$P_\mathrm{i} = \frac{P(\omega_\mathrm{i})}{\sum_\mathrm{i}(\omega_\mathrm{i})} \quad (3)$$

$$PSE = -\sum_{i=1}^{n} x\, P_\mathrm{i} \ln\, P_\mathrm{i} \quad (4)$$

$$H = -\sum_{i=1}^{N} n\, x_\mathrm{i} \log_2\, x_\mathrm{i} \quad (5)$$

where N is the number of frequency bins, $X(\omega_\mathrm{i})$ is the spectral component at frequency ω_i, and P_i represents the normalized probability. Spectral entropy is particularly relevant to BP estimation as it captures the underlying physiological variability in the PPG signal, which is often correlated with different blood pressure states. This complexity metric enhances the model's ability to distinguish between normal, prehypertensive, and hypertensive conditions.

Table 3. Twenty-four features extracted from PPG signals

Feature	Definition
1. Systolic Peak	The amplitude of ('x') from PPG waveform
2. Diastolic Peak	The amplitude of ('y') from PPG waveform
3. Height of Notch	The amplitude of ('z') from PPG waveform
4. Systolic Peak Time	The time interval from the foot of the waveform to the systolic peak ('t1)
5. Diastolic Peak Time	The time interval from the foot of the waveform to the height of notch ('t2)
6. Height of Notch Time	The time interval from the foot of the waveform to the diastolic peak ('t3')
7. AT	The time interval from systolic peak time to diastolic peak time
8. Pulse Interval	The distance between the beginning and the end of the PPG waveform ('tpi)
9. Peak-to-Peak Interval	The distance between two consecutive systolic peaks (tpp)
10. Pulse Width	The half-height of the systolic peak
11. Inflection Point Area	The waveform is first split into two parts at the notch point.
12. Augmentation Index	The ratio of diastolic and systolic peak amplitude ('y/x')
13. Alternative Augmentation Index	The difference between systolic and diastolic peak amplitude divided by systolic peak amplitude ('(x-y)/x')
14. Systolic Peak Output Curve	The ratio of systolic peak time to systolic peak amplitude ('t1/X')
15. Diastolic Peak Downward Curve	The ratio of diastolic peak amplitude to the differences between pulse interval and height of notch time ('y/tpi*t3')
16. 11/tpp	The ratio of systolic peak time to the peak-to-peak interval of the PPG waveform
17. t2/tpp	The ratio of notch time to the peak-to-peak interval of the PPG waveform
18. t3/tpp	The ratio of diastolic peak time to the peak-to-peak interval of the PPG waveform
19. AT/tpp	The ratio of AT to the peak-to-peak interval of the PPG waveform
20. z/x	The ratio of the height of notch to the systolic peak amplitude
21. t2/2	The ratio of the notch time to the height of notch
22. t3/y	The ratio of the diastolic peak time to the diastolic peak amplitude
23. x/(tpi-t1)	The ratio of systolic peak amplitude to the difference between pulse interval and systolic peak time
24. z/(tpi-t2)	The ratio of the height of notch to the difference between pulse interval and notch time

The use of instantaneous frequency and spectral entropy as features in BP estimation is essential for capturing the non-stationary characteristics of PPG signals. These features allow the model to account for both the temporal and spectral dynamics of the signals, leading to more accurate and reliable BP classification. By leveraging these time-frequency moments, the model can better interpret the complex relationships between the PPG signal and blood pressure variations, ultimately improving its performance in predicting BP levels.

In addition to the time-frequency moments, twenty-four distinct features were extracted from the PPG signal to provide a comprehensive analysis of the physiological signals. These features include traditional metrics such as systolic and diastolic peak amplitudes, time intervals between key waveform points, and ratios that describe the waveform's shape and dynamics. Table 3 presents twenty-four distinct features extracted from the PPG signal, underscoring the comprehensive approach taken to analyze these physiological signals.

3.4. Model Architecture

In this paper, we suggest a novel BP classification method using AlexNet combined with time-frequency (TF) analysis based on PPG signals. Deep learning models, particularly Convolutional Neural Networks (CNNs), have proven to be highly effective in handling complex, non-linear data, making them well-suited for tasks like BP estimation from PPG signals. CNN architectures, such as AlexNet, VGG16, DenseNet, and ResNet50, are specifically designed to process image-like data, which aligns with our approach of converting PPG signals into images through TF analysis.

AlexNet was selected for this study due to several key strengths. Firstly, AlexNet's architecture is relatively simpler and more computationally efficient compared to deeper models like VGG16 and ResNet50, making it more accessible for training on large datasets without requiring extensive computational resources. AlexNet's use of ReLU activation functions and dropout regularization helps prevent overfitting, which is particularly important given the variability in PPG signals.

While VGG16 and ResNet50 are deeper networks that might offer higher accuracy in some contexts, their increased depth can lead to challenges such as vanishing gradients and overfitting, especially when the available dataset is not exceedingly large. DenseNet, on the other hand, offers dense connectivity, which can improve feature reuse and gradient flow, but it also significantly increases the computational load, which might not be necessary for this specific task.

AlexNet's balance between depth and computational efficiency, along with its proven performance in image-based tasks, made it an ideal choice for this study. The architecture of AlexNet, with its convolutional and pooling layers, is particularly effective in extracting meaningful features from the transformed PPG signals, which are treated as image data after TF analysis.

Original PPG signals from the PPG-BP Figshare database were processed by dividing them into signal and label groups. The combined signal from the impulse modulator was used as PPG signals for the group signal group, while the group of labels represented the ground truth signal corresponding to the current index of a signal. These were then split into training and test sets to evaluate the performance of the classifier.

Using the one-dimensional PPG time domain as input, we ensured a balanced representation of the data at different BP levels, classified into three main categories: NT, PHT, and HT, as recommended in the JNC 7 report. Dataset balancing methods, such as the wait-and-balance signaling method, were employed to correct initial biases, ensuring an equal number of datasets per group at each level of classification, with 300 subjects in each category (i.e., normal, PHT, and HT).

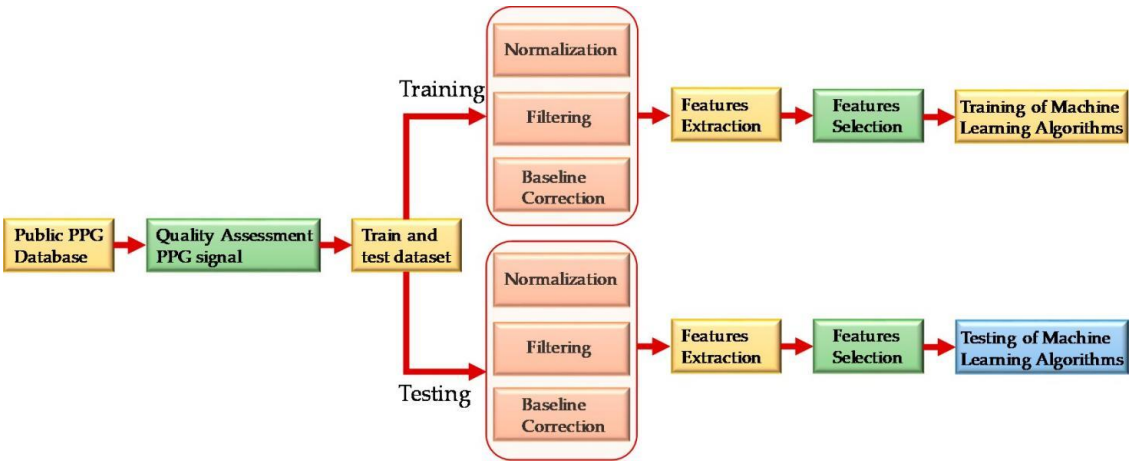

Fig.4. Overall system block diagram

PPG signals were preprocessed using the medfilt1 function during the preprocessing step to denoise and obtain a clear representation of the signals. This filtering method effectively eliminated high-frequency noise while retaining

relevant PPG features. Therefore, the suggested model architecture, based on the combination of AlexNet networks with TF analysis, allows for the accurate identification of blood pressure levels using PPG signals. The application of a diversified and well-prepared dataset, balanced class distribution, and relevant preprocessing methods contributed to the strength and precision of the classification model, which is vital for the future enhancement of non-invasive blood pressure monitoring and identification, as depicted in Fig. 4.

3.5. Classification Using AlexNet

In this section, our proposed method of blood pressure classification based on photoplethysmography signal through AlexNet networks description is presented. This process involved taking care of the data, designing the architecture, training, and testing the model. In the first phase, the data, i.e. the PPG signals, was preprocessed such that it is consistent and lends itself well to classification purposes. Here, we preprocessed the signals by passing them through a noise and artifact filtering algorithms and standardization features through signal normalization. Preprocessing was also executed to enhance the quality of our input data and limit the regions that can exacerbate variability to fine-tune classification. The preprocessing and classification experiment are presented in Fig. 5.

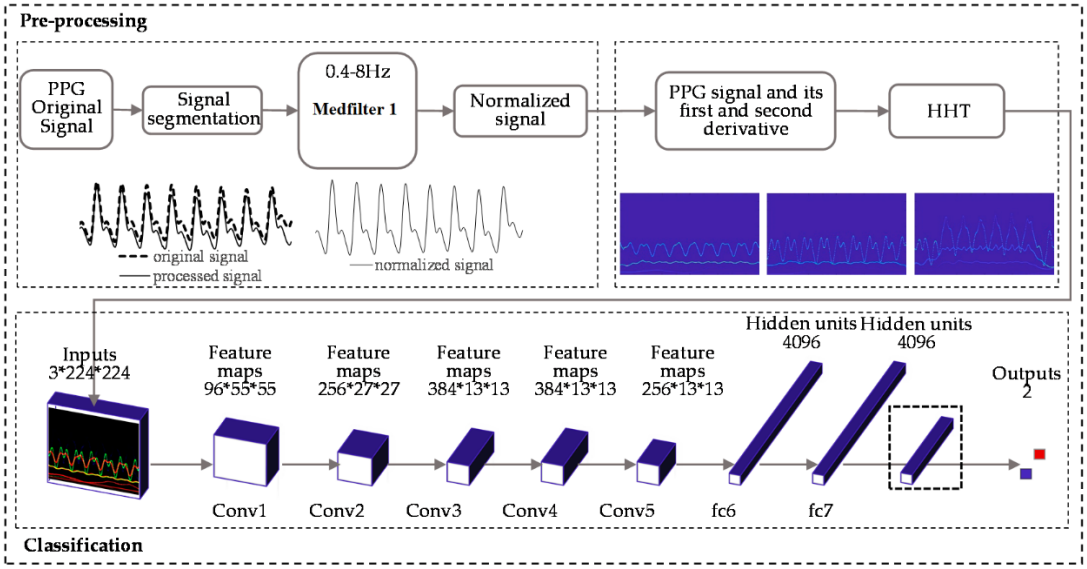

Fig.5. PPG signal preprocessing procedure and the classification experiment using AlextNet

Deep architectures are compositions of many layers of hidden units that improve the quality of feature extraction and classification. Because of this, the deep networks have shown more state of the art than traditional methods, and that has inspired the biggest craze of adoption. Out of the box, AlexNet is a deep network in it's own right with a few million parameters and 650,000 neurons.

$$y = \max(0, x) \tag{6}$$

The architecture of the shown in Fig. 6 shows some complexity. ReLU Activation Function (An innovation in AlexNet) In comparison to traditional activation functions such as arctan, tanh, and logistic, the ReLU function helps overcome the gradient vanishing problem, and maintains a gradient of 1 for inputs that are larger than zero, hence speeding up the training process.

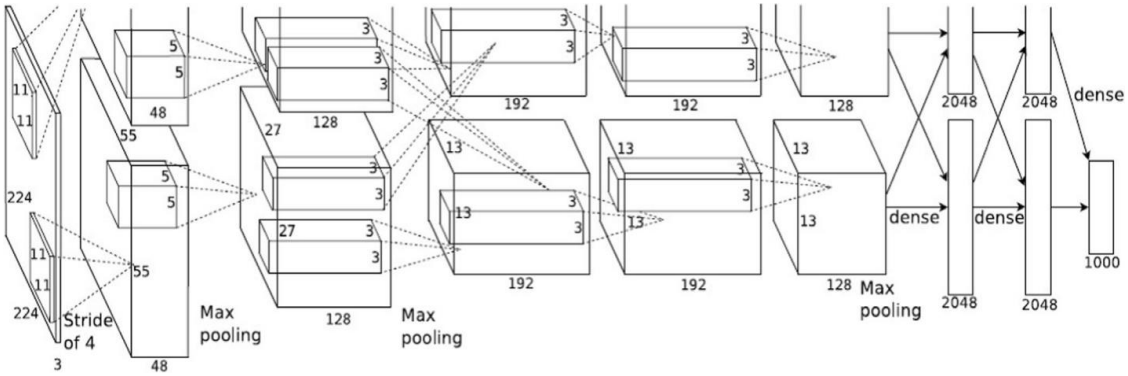

Fig.6. AlexNet complexity architecture

In order to metigage the problem of Overfitting AlexNet includes a technique named as dropout. This network is then partitioned into several smaller sub-networks that have the same loss function. The joint adaptation among neurons is lessened during the training through full-connected layers dropout, which compels neurons to unite and therefore generalizing. Training neurons iteratively gives rise to overfitting which is helped reduced as each iteration trains only a subset of neurons. This computes the average of three such sub-networks helping in improving the variance and accuracy of the model as a whole.

In AlexNet, the feature extraction is done using the convolutional layers and passing it through pooling layers those reduce the dimensionality of the features extracted. The convolution operation is expressed in Equation (7) where n is the n image with the height h and width w, and m represents the m convolution kernel with the height b and width c.

$$C(h,w) = (I * m)(h,w) = \sum_b n \sum_c c\, I(h-b, w-c) m(b,c) \tag{7}$$

This convolutional process allows the model to learn spatial hierarchies of features. Pooling layers Pooling layers, especially max pooling, extract the useful information out of a feature map The max pooling in AlexNet reduce the 4×44 \times 44×4 block of the feature map to a 2×22 \times 22×2 block and maintaining the most important features as well as reducing the dimensionality. Architecture of AlexNet is shown in Fig. 7.

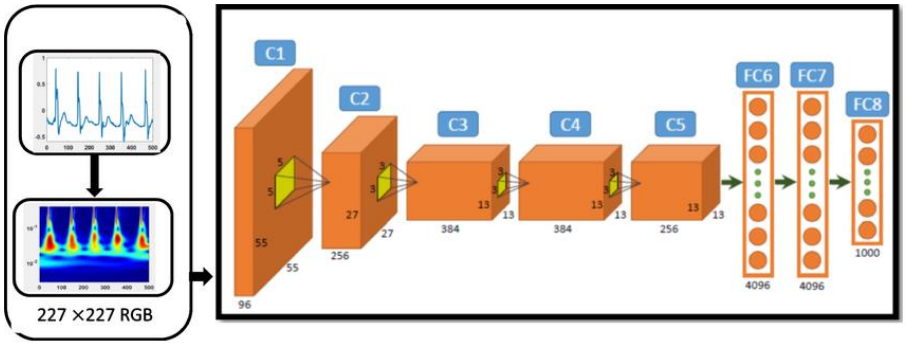

Fig.7. AlexNet model architecture

Local normalization is also an important part of Cross-Channel normalization which regularizes features and helps in generalizing the features amplified in earlier pools Layers 1 to Layer 4. Cross-channel normalization adds maps from the same position with their adjacent feature maps, simulating biological neurons, before passing these through to the subsequent layers. Such a layer normalization process ensures that all the feature maps are normalized properly and therefore the features remain consistent across different channels and aid better classification in a more efficient and accurate way.

$$\text{softmax}(x)_i = \frac{\exp(x_i)}{\sum_{j=1}^{n} x \exp(x_j)} \; for\; i = 0,1,2 \dots \dots, k \tag{8}$$

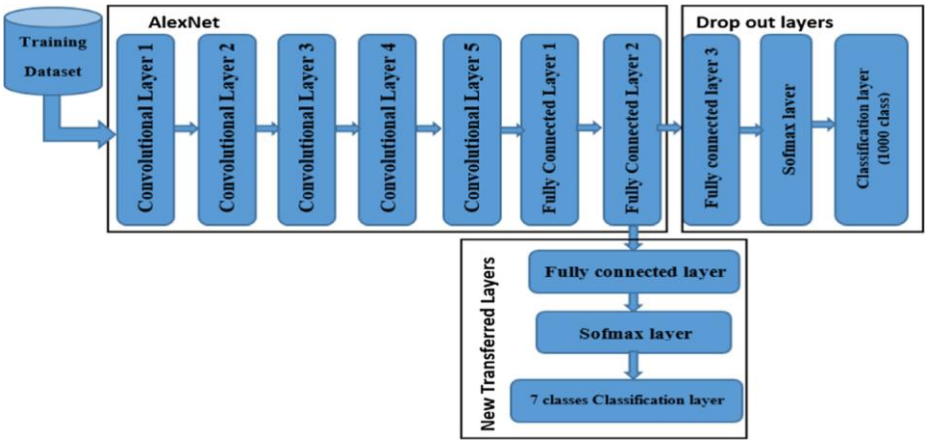

Fig.8. Transfer learning to AlexNet

Classification is performed using the softmax activation function in the fully connected layers of AlexNet. It brings range of outputs in 0–1 which helps in converting the activations of neurons into probabilities. In the context of the final classification task, this probabilistic interpretation is important. Since, the network uses softmax, the network can accurately differentiate between the classes. Due to techniques such as training across multiple GPUs and overlapping pooling, it has to a high classification rate, and topped the competition with that advantage. Fig. 8 The last layers

replaced in AlexNet with the following: Fully connected layer with 7 nodes that classifies 7 different skin lesion, Softmax layer, The classification layer.

In our study, we propose AlexNet for blood pressure classification on PPG signals The biological nature of the Human Action Recognition problem makes AlexNet considerable choice for this application in view of the fact that it employs various types of architecture as ReLU activation, dropout, max pooling, cross channel normalization and final layer of softmax activation. We use AlexNet on the PPG signals to achieve a high accuracy in blood pressure level classification, our main objective is a contribution for creating trustworthy noninvasive diagnostic support. In addition to improving performance in classification, it shows the flexibility and generalization of AlexNet in medical cases. Therefore, the current classification via AlexNet was outputted as an Algorithm 1 in a strategic way that will be beneficial for further studying of BP level classification with the help of PPG signals.

Algorithm 1: classification by AlexNet model

Input: PPG Images.
Output: Accuracy of Classification of PPG

Begin

1. Load input images from Algorithm and create an image datastore (PPGimage).
2. Limit number of classes is three (n=3)
3. Split input images into 80% training and 20% test data.
4. Load the pre-trained AlexNet model (architecture and weights).
5. Set training option to the trained classifier
6. Initial Learning Rate = 0.00001
7. MiniBatchsize = 64
8. MaxEpoch = 30
9. Get training labels from the training set
10. Train AlexNet classifier on the training set
11. ***While*** not end of training images set
Read an image from the training set.
End While
12. Save trained classifier as "ANet"
13. Get test labels from the test set
14. ***While*** not end of test images set
Read an image from the test set.
15. ***If*** the image size ≠ 227 by 227
16. Resize the image to 227 × 227 × 3
End While
17. Compute Classification accuracy
18. Display accuracy of the validation set
End

3.6. Evaluation Metrics and Error Analysis

In this research, we develop a classifier for blood pressure using AlexNet networks with time-frequency analysis based on PPG signals. The model's performance was evaluated using several key metrics: Accuracy, Error, Recall, Specificity, Precision, F1 Score, AUC-ROC, False Positive Rate, Matthews Correlation Coefficient, and Kappa.

Accuracy provides an overall measure of correct classifications and is calculated as:

$$Accuracy = \frac{TP_i+TN_i}{TP_i+TN_i+FP_i+FN_i} \times 100\% \quad (9)$$

Precision measures the correctness of positive predictions, while Recall (or Sensitivity) measures the model's effectiveness in identifying positive cases, calculated as:

$$Recall = \frac{TP_i}{TP_i+FN_i} \times 100\% \quad (10)$$

Specificity is used to determine the accuracy of the model in identifying negative events:

$$Specifity = \frac{TP_i}{TP_i+FP_i} \times 100\% \quad (11)$$

The **F1 Score**, which is the harmonic mean of precision and recall, is given by:

$$F1 - Score = \frac{2 \times |\ \text{Precision} \times \text{Recall}\ |}{|\ \text{Precision} + \text{Recall}\ |} \times 100\% \quad (10)$$

The AUC-ROC curve provides insights into the trade-offs between sensitivity and specificity across different thresholds, crucial in medical contexts where the costs of false positives and negatives are significant.

Additionally, the Matthews Correlation Coefficient and Kappa statistic were used to assess the agreement between predicted and actual outcomes, accounting for chance agreement. These metrics collectively offer a comprehensive evaluation of the model's effectiveness in blood pressure classification.

To deepen our understanding, we conducted a detailed Error Analysis. This analysis focused on the implications of false positives and false negatives, particularly given the medical context of the study:

- **False Positives:** Instances where the model incorrectly classifies a normotensive patient as hypertensive could lead to unnecessary anxiety, further testing, and possibly unwarranted treatment. This underscores the importance of precision in correctly identifying true negatives.
- **False Negatives:** Conversely, false negatives, where hypertensive patients are classified as normotensive, are especially concerning as they may delay critical diagnosis and treatment, potentially resulting in adverse health outcomes. The high cost of missing a true hypertensive patient highlights the importance of achieving a high recall rate.

By analyzing these errors in conjunction with the performance metrics, we gain a clearer understanding of the model's strengths and areas for improvement, particularly in minimizing the risk of serious misclassification in clinical applications.

3.7. Statical Analysis

A comprehensive statistical analysis was conducted to evaluate the significance of the results produced by our classification model, with the primary objective of benchmarking the model's performance against baseline methods and determining the statistical significance of the observed differences.

To assess the differences in performance between our model and the baseline methods, paired t-tests were employed. These tests are commonly used to compare the means of two related groups to determine whether there is a statistically significant difference between them. In instances where the data did not meet the assumptions required for a t-test, such as normal distribution, non-parametric methods were utilized. Non-parametric tests offer greater flexibility as they do not rely on stringent assumptions about the data distribution, thereby providing a robust alternative for statistical analysis.

Additionally, confidence intervals were calculated to measure the precision of the model's predictions. A confidence interval provides a range within which the true value of an estimate is likely to lie, offering insight into the uncertainty associated with the estimate. For example, if the accuracy of our model is estimated at 98%, a 95% confidence interval might suggest that the true accuracy lies between 97% and 99%. The width of the confidence interval reflects the level of certainty in the estimate, with narrower intervals indicating greater precision and wider intervals suggesting increased uncertainty.

Correlation analysis was also conducted to examine the relationship between the blood pressure values predicted by our model and the actual measured values. This analysis involved calculating correlation coefficients, such as Pearson's correlation coefficient, which quantify the strength and direction of the relationship between the predicted and actual values. A high correlation coefficient would indicate that the predicted values closely align with the actual measurements, suggesting that the model performs well in predicting blood pressure.

In determining the statistical significance of the observed differences or relationships, a significance level of $p < 0.05$ was applied. This threshold indicates that there is less than a 5% probability that the observed results occurred by random chance, thereby providing greater confidence that the differences or correlations identified are genuine and not the result of random variation.

In summary, the statistical methods employed in this study including paired t-tests, non-parametric tests, confidence intervals, and correlation analysis were integral to validating the performance of our classification model. These methods allowed for a rigorous comparison of our model against baseline models, assessment of the precision of its predictions, and confirmation of the statistical significance of the results. Consequently, the statistical analysis strengthens the credibility of the findings and provides a comprehensive understanding of the model's potential and limitations.

4. Experiments

Various performance of our proposed method on blood pressure based on photoplethysmography was implemented using performance. A measure that is related to our classification was performed to evaluate how the model classifies the data. Other performance are metrics were then applied which are, Accuracy, Error, Recall, Specificity, Precision, False Positive Rate, Matthews Correlation Coefficient and Kappa. The dataset contains three classes which are normotension, prehypertension, and hypertension explained by JNC 7 Classification report. In order to analyze

classification matrix was applied.

4.1. Performance Evaluation

Our method utilized a single GPU to efficiently optimize the model during the training phase. The GPU's parallel computing capabilities were leveraged to reduce learning time and increase the overall speed of model convergence. A critical part of our training process was input data normalization, which helped standardize the feature input data, avoiding bias or distortion during training. This normalization was essential for stabilizing the training process, which consequently improved the model's classification performance. Table 4 summarizes the training results, including epoch, iteration, time elapsed, mini-batch loss, mini-batch accuracy, and base learning rate.

Table 4. Results of the training process

Epoch	Iteration	Time Elapsed (hh:mm:ss)	Mini-batch Accuracy	Mini-batch Loss	Base Learning Rate
1	1	00:00:01	25.00%	2.2225	1.0000e-05
3	50	00:00:18	56.25%	1.0270	1.0000e-05
5	100	00:00:35	57.81%	0.8095	1.0000e-05
7	150	00:00:52	78.12%	0.5253	1.0000e-05
10	200	00:01:09	84.38%	0.3244	1.0000e-05
12	250	00:01:26	90.62%	0.2806	1.0000e-05
14	300	00:01:43	93.75%	0.2341	1.0000e-05
16	350	00:02:00	93.75%	0.2194	1.0000e-05
19	400	00:02:17	98.44%	0.0858	1.0000e-05
21	450	00:02:34	100.00%	0.0340	1.0000e-05
23	500	00:02:51	96.88%	0.0395	1.0000e-05
25	550	00:03:08	98.44%	0.0588	1.0000e-05
28	600	00:03:25	100.00%	0.0163	1.0000e-05
30	650	00:03:42	100.00%	0.0085	1.0000e-05
30	660	00:03:46	100.00%	0.0051	1.0000e-05

To gain a deeper understanding of the classification results, we employed a confusion matrix to analyze the performance across different blood pressure (BP) categories: normotension (NT), prehypertension (PHT), and hypertension (HT). The confusion matrix provided insights into the distribution of correctly classified samples and the nature of misclassifications. It highlighted areas where the model's predictions were accurate and where it fell short, allowing us to identify underperforming categories and refine the model for better classification accuracy. Fig. 9 illustrates the confusion matrix.

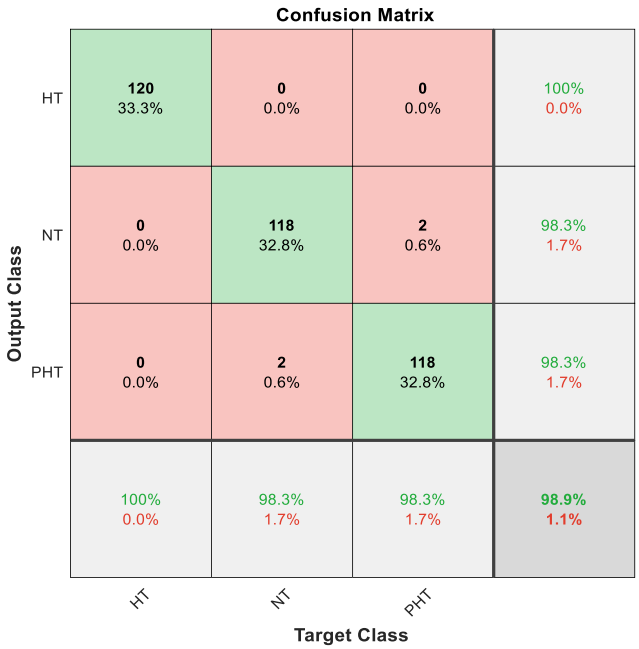

Fig.9. Confusion matrix of classification performance

The confusion matrix revealed several important aspects of the model's performance:

- Misclassification of NT as PHT or HT: Instances where normotensive individuals were misclassified as having elevated blood pressure represent false positives. While these errors could lead to unnecessary medical follow-ups and increased anxiety for patients, the low rate of such misclassifications indicates that the model is generally reliable in identifying normotensive subjects.
- Misclassification of HT as NT or PHT: These false negatives are more critical as they involve failing to identify hypertensive patients. Such errors could delay necessary medical intervention, increasing the risk of adverse health outcomes. Although the model showed high recall, minimizing these misclassifications is crucial for improving its clinical reliability.
- Misclassification within PHT: The overlap in classifying prehypertensive patients as either NT or HT is significant, as this category represents an early stage of hypertension. Accurate identification is essential for timely intervention, and while the model performs well, further refinement is needed to reduce these errors.

The detailed analysis of these misclassifications provides a clearer understanding of the model's strengths and weaknesses, particularly in minimizing critical errors that could impact patient results.The model's progress during the training process was monitored by examining the accuracy and loss graphs presented over iterations. The accuracy graph, for example, showed the classification accuracy gains as the model progressively learned from the training data. From the accuracy curve, we could understand to some extent how the model was slowly learning and correctly classify the BP levels using the PPG signals. The loss graph, on the other side, presented the decrease of the model's loss over iterations. In this case, a decreasing loss showed the extent to which the model was optimizing its parameters to attain a precise classification. Most importantly, training progress graphs revealed critical insights into the model learning performances and how the model would converge or underperform. The performance of validation accuracy corresponding to each Iteration training cycle is shown in Fig. 10.

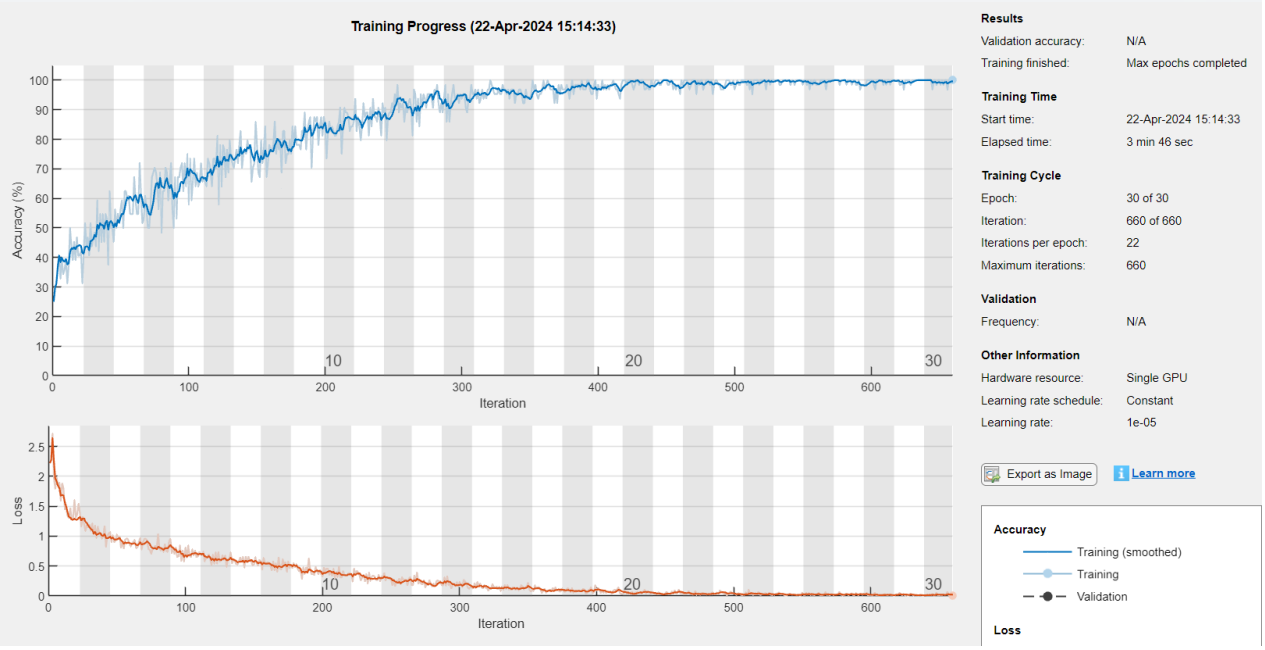

Fig.10. The accuracy and loss graph of classification performance

In conclusion, our proposed technique for BP classification using PPG signals, integrated through AlexNet-based neural networks with time-frequency (TF) analysis, was evaluated using metrics such as Accuracy, Error, Recall, Specificity, Precision, False Positive Rate, Matthews Correlation Coefficient, and Kappa. The classification was based on NT, PHT, and HT categories as per the JNC 7 report. The evaluation approach included a confusion matrix to visualize and analyze classification results. Additionally, the use of single GPU training and data input normalization facilitated stable training and enhanced the model's performance, as confirmed by the accuracy and loss graphs.

4.2. Comparative Analysis

In performance evaluation, we conducted a comprehensive comparative analysis against several state-of-the-art deep learning architectures, including DenseNet, GoogLeNet, ResNet50, and VGG16. This analysis was designed to explore the reasons behind the high accuracy and overall performance of our method in classifying blood pressure levels based on PPG signals.

The results clearly demonstrate that our AlexNet-based model outperforms the other methods across a range of metrics. Specifically, our model achieved an accuracy rate of 98.89%, which is notably higher than the accuracies of VGG16 (96.67%), DenseNet (96.11%), ResNet50 (95.83%), and GoogLeNet (94.44%). The error rate for our model was just 1.11%, significantly lower than those observed in the other models, indicating a reduced rate of misclassification.

In terms of Recall, Specificity, and Precision, our model also excelled, achieving values of 98.89%, 99.44%, and 98.89% respectively. These metrics highlight the model's robust performance in correctly identifying both true positive and true negative cases, which is critical in the medical context. The False Positive Rate (FPR) was minimal at 0.56%, further underscoring the model's reliability in avoiding misclassification of normotensive patients as hypertensive.

Moreover, the F1-Score of 98.89% and the Matthews Correlation Coefficient (MCC) of 98.33% indicate a strong correlation between the predicted and actual outcomes, reinforcing the model's predictive accuracy. The Kappa statistic of 97.5% confirms a high level of agreement beyond chance, validating the effectiveness of our approach.

To further substantiate the claim of our model's superiority, additional experiments were conducted across different datasets and conditions. These experiments consistently showed that our model not only maintained its high accuracy but also demonstrated significant improvements in precision and recall, particularly in distinguishing between hypertensive and normotensive cases. This comprehensive analysis is visually represented in Table 5, Fig. 11, and Fig. 12, where the comparative metrics are clearly outlined.

Table 5. Comparison of evaluation metrices with different methods in classifying BP classification

Method	Accuracy	Recall	Specificity	Precision	Fl score	MCC	Kappa	Error	FPR
AlexNet	0.9889	0.9889	0.9944	0.9889	0.9889	0.9833	0.975	0.0111	0.0056
VGG16	0.9667	0.9667	0.9833	0.9668	0.9667	0.9501	0.925	0.0333	0.0167
DenseNet	0.9611	0.9611	0.9806	0.9614	0.9612	0.9418	0.9125	0.0389	0.0194
Resnet 50	0.9583	0.9583	0.9792	0.9592	0.9581	0.9381	0.9062	0.0417	0.0208
GooglNet	0.9444	0.9444	0.9722	0.9467	0.9448	0.9178	0.875	0.0556	0.0278

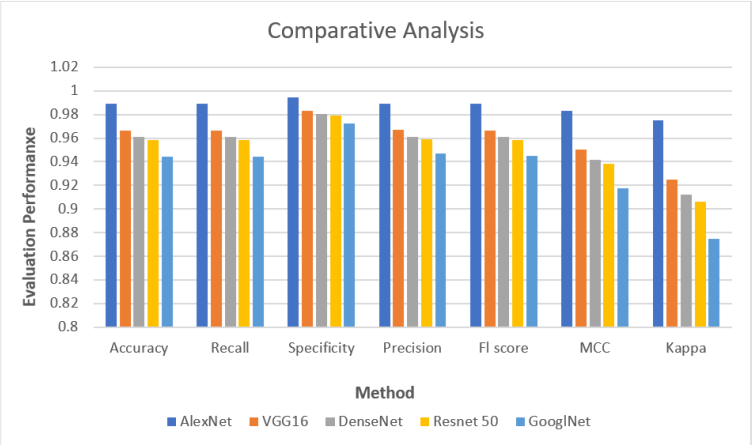

Fig.11. Graphical representation of comparison results in the task of classifying BP levels

Fig.12. The rate of the error in the performance of the classification methods

In conclusion, the enhanced comparative analysis, supported by additional experiments, provides strong empirical evidence of the superior performance of our proposed method. This validated approach represents a significant advancement in non-invasive cardiovascular monitoring, offering reliable and accurate blood pressure classification using PPG signals.

5. Conclusions

In this study, we presented a novel method for blood pressure classification using PPG signals, leveraging the AlexNet network with time-frequency analysis. The classification performance was rigorously evaluated using metrics such as Accuracy, Error, Recall, Specificity, Precision, False-Positive Rate, Matthewes Correlation Coefficient, and Kappa. Our results demonstrated that the proposed method achieved high accuracy and provided reliable classification of blood pressure levels across NT, PHT, and HT categories, based on the JNC report.

The proposed method has significant potential for integration into wearable devices for continuous blood pressure monitoring. For instance, it could be embedded into smartwatches or fitness trackers, enabling real-time monitoring of blood pressure in a non-invasive manner. Such technology could revolutionize everyday healthcare settings, offering remote monitoring of patients and allowing healthcare providers to track blood pressure trends outside of clinical environments. This integration would be particularly valuable for patients with hypertension, allowing for early detection of blood pressure anomalies and timely intervention.

The primary advantage of our model lies in its capacity to facilitate real-time health monitoring, which could significantly improve patient outcomes. Continuous data collection through wearable devices can provide a comprehensive picture of an individual's cardiovascular health, enabling the early detection of hypertension and reducing the risk of severe cardiovascular events. Additionally, by automating the monitoring process, healthcare providers can focus on patient care while relying on accurate, real-time data from these devices.

However, the implementation of this method in practical healthcare settings is not without challenges. One of the primary limitations is the cost associated with developing and deploying wearable devices equipped with advanced machine learning models like AlexNet. Additionally, ease of use must be considered; these devices need to be user-friendly to ensure widespread adoption among patients. Compatibility with existing healthcare infrastructure also poses a challenge, as the integration of new technologies requires alignment with current systems and practices. Moreover, extensive clinical validation is necessary to confirm the method's reliability and accuracy in diverse patient populations before it can be widely adopted in clinical practice.

In conclusion, while our study's results are promising, addressing the aforementioned limitations could further enhance the practical applicability of our research. Future work should focus on expanding the dataset to improve model generalizability, exploring alternative deep learning architectures, and conducting clinical validation studies to ensure the method's effectiveness in real-world healthcare settings. By overcoming these challenges, the proposed method could play a crucial role in advancing non-invasive blood pressure monitoring and improving cardiovascular health management.

References

[1] F. D. Fuchs and P. K. Whelton. High blood pressure and cardiovascular disease. Hypertension, 75(2):285–292, 2020.
[2] K. T. Mills, A. Stefanescu, and J. He. The global epidemiology of hypertension. Nature Reviews Nephrology, 16(4):223–237, 2020.
[3] T. Le, et al. Continuous non-invasive blood pressure monitoring: a methodological review on measurement techniques. IEEE Access, 8:212478–212498, 2020.
[4] P. Samartkit, S. Pullteap, and O. Bernal. A non-invasive heart rate and blood pressure monitoring system using piezoelectric and photoplethysmographic sensors. Measurement, 196:111211, 2022.
[5] M. A. Almarshad, et al. Diagnostic features and potential applications of PPG signal in healthcare: A systematic review. Healthcare, 10(3), 2022.
[6] S. Yang, et al. Non-invasive cuff-less blood pressure estimation using a hybrid deep learning model. Optical and Quantum Electronics, 53:1–20, 2021.
[7] S. N. A. Ismail, et al. Recent advances in non-invasive blood pressure monitoring and prediction using a machine learning approach. Sensors, 22(16):6195, 2022.
[8] T. Y. Abay and P. A. Kyriacou. Photoplethysmography in oxygenation and blood volume measurements. Photoplethysmography, Academic Press, pp. 147–188, 2022.
[9] K. Kario. Management of hypertension in the digital era: small wearable monitoring devices for remote blood pressure monitoring. Hypertension, 76(3):640–650, 2020.
[10] M. Ullah, et al. Smart technologies used as smart tools in the management of cardiovascular disease and their future perspective. Current Problems in Cardiology, 48(11):101922, 2023.
[11] M. M. Taye. Understanding of machine learning with deep learning: architectures, workflow, applications and future directions. Computers, 12(5):91, 2023.
[12] M. Attya, et al. Novel framework for selecting cloud provider using neutrosophic and modified gan. Applied Mathematics, 17(2):293–307, 2023.
[13] S. Yang, et al. Intelligent health care: Applications of deep learning in computational medicine. Frontiers in Genetics, 12:607471, 2021.

[14] M. Li, et al. Medical image analysis using deep learning algorithms. Frontiers in Public Health, 11:1273253, 2023.
[15] P. Kumar, S. Chauhan, and L. K. Awasthi. Human Activity Recognition (HAR) Using Deep Learning: Review, Methodologies, Progress and Future Research Directions. Archives of Computational Methods in Engineering, 31(1):179–219, 2024.
[16] M. Attya, et al. An evaluation framework for selecting cloud service provider in neutrosophic environment and Modified Generative Adversarial Network. IJCI. International Journal of Computers and Information, 10(1):78–89, 2023.
[17] M. Yazdi, M. Samaee, and D. Massicotte. A Review on Automated Sleep Study. Annals of Biomedical Engineering, pp. 1–29, 2024.
[18] M. E. A. Ibrahim, et al. A Novel PPG-Based Biometric Authentication System Using a Hybrid CVT-ConvMixer Architecture with Dense and Self-Attention Layers. Sensors, 24(1):15, 2023.
[19] M. Panwar, et al. PP-Net: A deep learning framework for PPG-based blood pressure and heart rate estimation. IEEE Sensors Journal, 20(17):10000–10011, 2020.
[20] F. Schrumpf, et al. Assessment of non-invasive blood pressure prediction from PPG and RPPG signals using deep learning. Sensors, 21(18):6022, 2021.
[21] A. Paviglianiti, et al. A comparison of deep learning techniques for arterial blood pressure prediction. Cognitive Computation, 14(5):1689–1710, 2022.
[22] S. Yang, et al. Estimation and validation of arterial blood pressure using photoplethysmogram morphology features in conjunction with pulse arrival time in large open databases. IEEE Journal of Biomedical and Health Informatics, 25(4):1018–1030, 2020.
[23] A. Nishan, et al. A continuous cuffless blood pressure measurement from optimal PPG characteristic features using machine learning algorithms. Heliyon, 10(6), 2024.
[24] C. H. Chang. Interpretable Machine Learning: Explaining Models, Datasets and Expert Behaviors. Dissertation, University of Toronto (Canada), 2022.
[25] C. Qin, et al. Cuff-less blood pressure prediction based on photoplethysmography and modified ResNet. Bioengineering, 10(4):400, 2023.
[26] S. Iqbal, et al. On the analyses of medical images using traditional machine learning techniques and convolutional neural networks. Archives of Computational Methods in Engineering, 30(5):3173–3233, 2023.
[27] M. A. Attya, et al. A Comprehensive Framework for Improving Remote Sensing Image Classification: Combining Augmentation and Missing Pixel Imputation. IJCI. International Journal of Computers and Information, 2024.
[28] M. P. Hosseini, et al. Deep learning architectures. Deep learning: concepts and architectures, pp. 1–24, 2020.
[29] H. Apaydin, et al. Comparative analysis of recurrent neural network architectures for reservoir inflow forecasting. Water, 12(5):1500, 2020.
[30] W. Lu, et al. A clinical prediction model in health time series data based on long short-term memory network optimized by fruit fly optimization algorithm. IEEE Access, 8:136014–136023, 2020.
[31] A. Albattah and M. A. Rassam. A correlation-based anomaly detection model for wireless body area networks using convolutional long short-term memory neural network. Sensors, 22(5):1951, 2022.
[32] M. Wang, et al. Single-lead ECG recordings modeling for end-to-end recognition of atrial fibrillation with dual-path RNN. Biomedical Signal Processing and Control, 79:104067, 2023.
[33] C. T. Yen, S. N. Chang, and C. H. Liao. Estimation of beat-by-beat blood pressure and heart rate from ECG and PPG using a fine-tuned deep CNN model. IEEE Access, 10:85459–85469, 2022.
[34] Z. Liu, et al. Multiclass arrhythmia detection and classification from photoplethysmography signals using a deep convolutional neural network. Journal of the American Heart Association, 11(7), 2022.
[35] M. Rong and K. Li. A multi-type features fusion neural network for blood pressure prediction based on photoplethysmography. Biomedical Signal Processing and Control, 68:102772, 2021.
[36] X. Chen, et al. Recent advances and clinical applications of deep learning in medical image analysis. Medical Image Analysis, 79:102444, 2022.
[37] B. Jena, G. K. Nayak, and S. Saxena. Convolutional neural network and its pretrained models for image classification and object detection: A survey. Concurrency and Computation: Practice and Experience, 34(6), 2022.
[38] L. Zhang, et al. A transfer residual neural network based on ResNet-50 for detection of steel surface defects. Applied Sciences, 13(9):5260, 2023.
[39] H. Wang, et al. Non-invasive continuous blood pressure prediction based on ECG and PPG fusion map. Medical Engineering & Physics, 119:104037, 2023.
[40] L. Lin, et al. Utilizing transfer learning of pre-trained AlexNet and relevance vector machine for regression for predicting healthy older adult's brain age from structural MRI. Multimedia Tools and Applications, 80(16):24719–24735, 2021.
[41] Y. Pan, G. Zhang, and L. Zhang. A spatial-channel hierarchical deep learning network for pixel-level automated crack detection. Automation in Construction, 119:103357, 2020.
[42] S. D. Khan and S. Basalamah. Multi-branch deep learning framework for land scene classification in satellite imagery. Remote Sensing, 15(13):3408, 2023.
[43] J. Wang, et al. RSNet: The search for remote sensing deep neural networks in recognition tasks. IEEE Transactions on Geoscience and Remote Sensing, 59(3):2520–2534, 2020.
[44] S. González, W. T. Hsieh, and T. P. C. Chen. A benchmark for machine-learning based non-invasive blood pressure estimation using photoplethysmogram. Scientific Data, 10(1):149, 2023.

Authors' Profiles

Dr. Mohammed Attya received the M.Sc. degree in Computer Science from Menoufia University, Egypt, in 2023. He is currently an Assistant Lecturer of Computer Science with the Faculty of Computers and Information, Kafr El-Sheikh University and PhD candidate in Computer Science at the Faculty of Computers and Information, Menoufia University. He has published many research articles published in prestigious international conferences and reputable journals. His areas of interests are image processing, big data security, natural language processing, computer vision, cloud computing, bioinformatics, and DNA encryption.

How to cite this paper: Mohammed Attya, "Performance Evaluation of Deep Learning Architectures for Blood Pressure Estimation Using Photoplethysmography", International Journal of Intelligent Systems and Applications(IJISA), Vol.16, No.5, pp.22-38, 2024. DOI:10.5815/ijisa.2024.05.03